

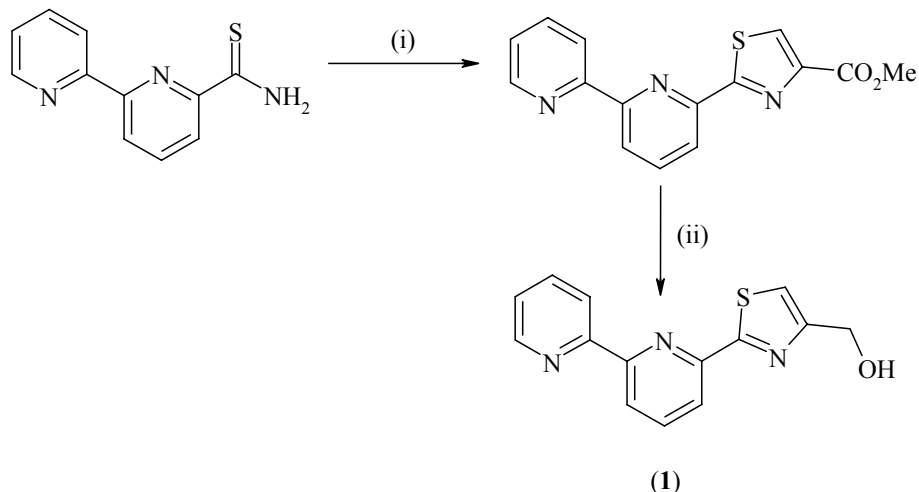
Isomeric Pyridyl-Thiazole Donor Units for Metal Ion Recognition in Bi- and Tri-metallic Helicates

Sam Bullock, Lisa J. Gillie, Lindsay P. Harding, Craig R. Rice, Thomas Riis-Johannessen and Martina Whitehead

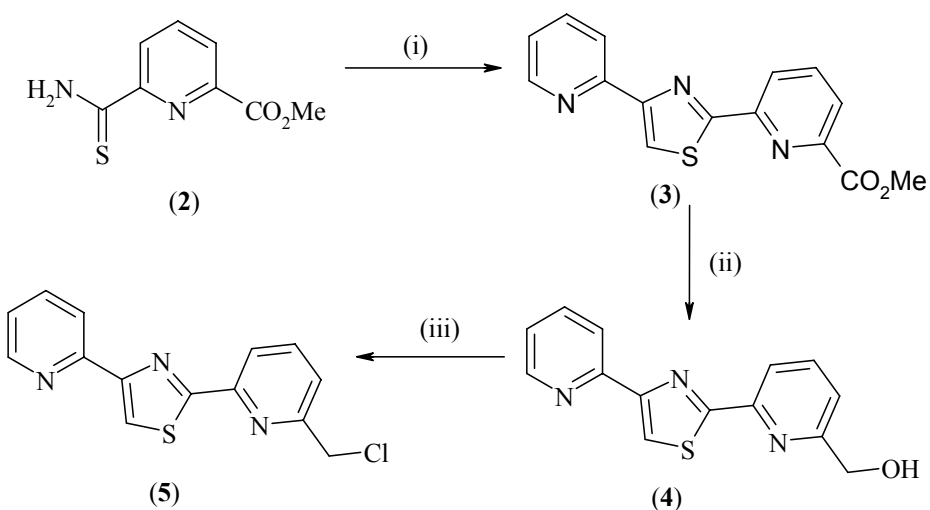
Electronic Supporting Information

Spectroscopic and Analytical Measurements. Automated spectrophotometric titrations were performed with a J&M diode array spectrometer (Tidas series) connected to an external computer. In a typical experiment, 50 mL of ligand ($2 \cdot 10^{-4}$ M) in MeCN + 0.01 M [Bu₄N][ClO₄] were titrated at 25 °C with Zn(ClO₄)₂·6H₂O or Hg(ClO₄)₂·4H₂O ($1 \cdot 10^{-3}$ M) in the same electrolyte solution under an inert atmosphere. After each addition of 0.2 mL, the absorbance was recorded using Hellma optrodes (optical path length 0.5 cm) immersed in the thermostated titration vessel and connected to the spectrometer. Mathematical treatment of the spectrophotometric data was performed with factor analysis and with the SPECFIT program.¹ ¹H and ¹³C NMR spectra were recorded at 25 °C on a Bruker Avance 400 MHz spectrometer. Chemical shifts are given in ppm with respect to CHD₂CN. Pneumatically-assisted electrospray (ESI-MS) mass spectra were recorded from 10^{-4} M solutions on a Finnigan SSQ7000 instrument.

Synthetic details for preparation of the ligands L¹, L³ and L⁴.



Scheme 1. Synthesis of the pyridine-pyridine-thiazole methanol derivative (1). Reagents and conditions: (i) ethyl bromopyruvate, EtOH, reflux (ii) NaBH₄, EtOH, reflux.²



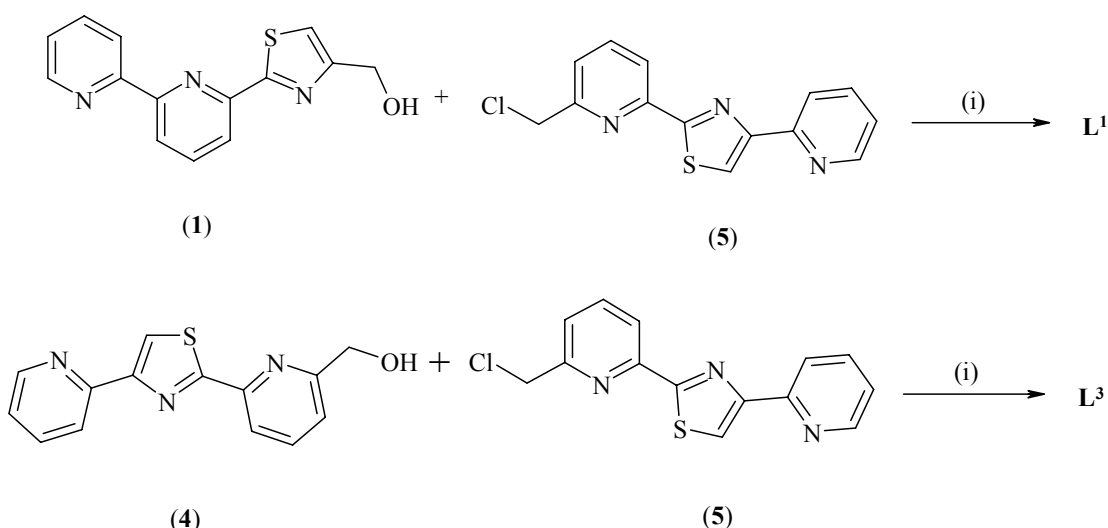
Scheme 2. Synthesis of pyridine-thiazole-pyridine methanol (**4**) and chloromethane (**5**) derivatives. Reagents and conditions: (i) α -bromoacetylpyridine, EtOH, reflux (ii) NaBH_4 , EtOH, reflux (iii) thionyl chloride, DCM, reflux.

Synthesis of the py-tz-py tridentate ester (**3**). To a solution of methylpicolinate-6-thioamide (1.0 g, 5.1 mmol) in EtOH (25ml) was added the hydrobromide salt of α -bromoacetyl pyridine (2.87 g, 10 mmol) and the solution refluxed for 6 hrs. The solution was then left to stand overnight during which time a precipitate formed, which was isolated by filtration giving the tridentate ester (**3**) as a tan solid (1.10 g, 73 %). ^1H NMR (400MHz, CDCl_3) δ 9.62 (s, 1H, tz), 8.96 (d, J = 5.6, 1H, py), 8.68 (d, J = 5.6, 1H, py), 8.61 (d, J = 7.8, 1H, py), 8.48 (dt, J = 7.8, 1.4, 1H, py), 8.20 (d, J = 6.8, 1H, py), 8.04 (t, J = 7.8, 1H, py), 7.84 (t, J = 7.2 Hz, 1H, py), 4.05 (s, 3H, - CH_3).

Synthesis of the the py-tz-py tridentate alcohol (**4**). To a solution of the ester (**3**) (1.0 g, 3.4 mmol) in EtOH (25 ml) was added NaBH_4 (0.38 g, 10.2 mmol) and the solution refluxed for 6 hrs. The reaction was monitored by TLC (Al_2O_3 1% MeOH in DCM) for consumption of the starting material and periodically more NaBH_4 was added if required. Upon completion the solvent was removed and the product partitioned between $\text{NaHCO}_{3(\text{aq})}$ and DCM, separation of the organic layer, drying and evaporation gave the alcohol (**4**) in sufficient purity to proceed to the next step (0.5 g, 55 %). ^1H NMR (400MHz, CDCl_3) δ 8.59 (m, 1H, py), 8.18 (m, 2H, overlapping, py), 8.14 (s, 1H, tz), 7.77 (t, J = 7.8, 1H, py), 7.75 (dt, J = 7.8, 1.8, 1H, py), 7.21 (m, 2H, overlapping, py), 4.77 (d, J = 5.0, 2H, - CH_2-), 3.67 (t, J = 5.1 Hz 1H, - CH_2OH).

Synthesis of the py-tz-py tridentate chloromethyl derivate (**5**). To a solution of the alcohol (**4**) (0.25 g, 0.9 mmol) in DCM (25 ml) was added Na_2CO_3 (1g) and thionyl chloride (0.6 g, 5 mmol) and the solution refluxed for 6 hrs. After this time the cooled reaction was carefully poured onto $\text{NaHCO}_{3(\text{aq})}$ and the organic layer separated, dried and evaporated. Purification by column chromatography (Al_2O_3 1% MeOH in DCM) giving the chloro derivative (**5**) as a colorless solid (0.19 g, 74 %). ^1H NMR (400MHz, CDCl_3) δ 8.58 (ddd, J = 4.8, 1.7, 0.9, 1H, py), 8.19 (t, J =

7.6, 1H, py), 8.13 (s, 1H, tz), 7.80 (t, J = 7.8, 1H, py), 7.74 (dt, J = 7.7, 1.8, 1H, py), 7.48 (d, J = 7.8, 1H, py), 7.19 (m, 1H, overlapping with CHCl_3) 4.68 (s, 2H, - CH_2Cl).



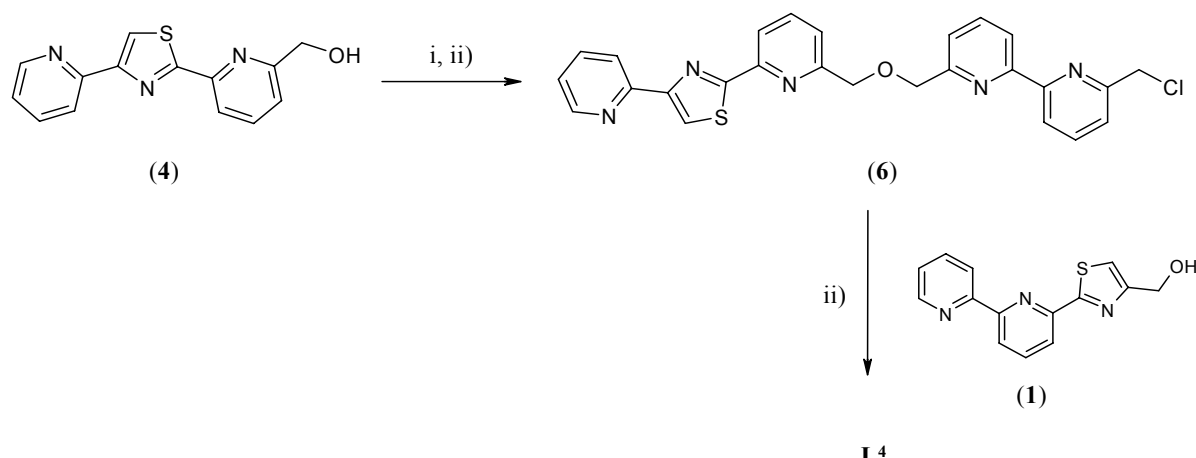
Scheme 3. Synthesis of ligands L^1 and L^3 . Reagents and conditions: (i) NaH , anhydrous THF, EtN_4I (cat), reflux.

Synthesis of ligands L^1 and L^3 . Both ligands were prepared in an analogous manner. In a typical procedure a solution of the alcohol (either **1** or **4**) and tetraethylammonium iodide (0.005 g, cat) in anhydrous THF, under dinitrogen, was added an excess of NaH (typically 2 equivalents) and the reaction heated to 50 °C for 1 hr. To this was added a solution of one equivalent of the chloro derivative (**5**) in THF and the reaction refluxed. The reaction was monitored by TLC (Al_2O_3 5% MeOH in DCM) until the choloro derivative had disappeared. The reaction was then cooled, methanol added (to react with any remaining NaH) and evaporated. Purification by column chromatography (Al_2O_3 5% MeOH in DCM) gave ligands L^1 or L^3 .

Yield 55%. L^1 : ^1H NMR (400MHz, CDCl_3) δ 8.70 (ddd, J = 4.8, 1.8, 0.9, 1H, py), 8.65 (ddd, J = 4.8, 1.8, 1.0, 1H, py), 8.57 (dt, J = 8.0, 1.0, 1H, py), 8.47 (dd, J = 7.9, 1.0, 1H, py), 8.24 (m, 3H, overlap, py), 8.18 (s, 1H, tz), 7.93 (t, J = 7.8, 1H, py), 7.87 (m, 2H, overlap, py), 7.81 (dt, J = 7.7, 1.8, 1H, py), 7.61 (d, J = 7.3, 1H, py), 7.48 (s, 1H, tz), 7.35 (ddd, J = 7.5, 4.8, 1.2 Hz, 1H, py), 7.26 (m, 1H, overlap with CHCl_3 , py), 4.85 (s, 2H, - CH_2-) 4.82 (s, 2H, - CH_2-). ^{13}C (125 MHz, CDCl_3) 169.8, 169.1, 158.6, 156.5, 155.8, 155.4, 155.0, 150.7, 150.6, 149.5, 149.1, 145.4, 143.3, 137.9, 137.6, 136.9, 124.0, 122.8, 122.5, 121.7, 121.3, 121.1, 119.6, 119.4, 118.7, 118.4, 73.3 (- $\text{CH}_2\text{O}-$), 69.0 (- $\text{CH}_2\text{O}-$). ESI-MS m/z 521 ($\text{M} + \text{H}^+$).

Yield 61%. L^3 : ^1H NMR (400MHz, CDCl_3) δ 8.65 (d, J = 4.8, 2H, py), 8.26 (d, J = 5.3, 2H, py), 8.24 (d, J = 5.0, 2H, py), 8.18 (s, 2H, tz), 7.88 (t, J = 7.7, 2H, py), 7.81 (dt, J = 7.7, 1.7, 2H, py), 7.64 (d, J = 7.6 Hz, 2H, py), 7.19 (m, 2H, overlap with CHCl_3 , py), 4.85 (s, 4H, - CH_2-). ^{13}C (125

MHz, CDCl₃) 169.2, 158.5, 152.6, 150.7, 149.4, 137.6, 137.0, 122.8, 122.2, 121.1, 119.6, 118.5, 116.1, 73.6 (-CH₂O-). ESI-MS *m/z* 521 (M + H⁺).



Scheme 4. Synthesis L⁴. Reagents and conditions: (i) 2,2'-bipyridine-6,6'-dichloromethanol (ii) NaH, anhydrous THF, EtN₄I, reflux.

Synthesis of (6). To a solution of py-tz-py tridentate alcohol (**4**) (0.05 g, 0.18 mmol) and tetraethylammonium iodide (0.005 g) in anhydrous THF (25 ml), under dinitrogen was added NaH (0.007 g, 0.29 mmol) and the reaction stirred at 50°C for 1 hr. To this was then added a solution of 2,2'-bipyridine-6,6'-dichloromethyl³ (0.037 g, 0.16 mmol) in THF and the reaction was refluxed. The reaction was monitored by TLC (Al₂O₃ 1% MeOH in DCM) and once all the dichloro derivative had been consumed the reaction was cooled, evaporated and purified by column chromatography (Al₂O₃ 1% MeOH in DCM) giving (**6**) as a colourless solid (0.06 g, 73 %). ¹H NMR (400MHz, CDCl₃) δ 8.30 (dd, *J* = 7.6, 2.0, 1H, py), 8.58 (m, 2H overlapping, py), 8.17 (t, *J* = 9.0, 2H), 8.11 (s, 1H, tz), 7.80 (dd, *J* = 7.7, 3.4, 1H, py), 7.76 (m, 3H, overlapping, py), 7.54 (t, *J* = 6.7, 2H, py), 7.43 (d, *J* = 5.3 Hz, 1H, py), 7.19 (m, overlapping with CHCl₃, 1H), 4.85 (s, 2H, -CH₂-), 4.83 (s, 2H, -CH₂-), 4.69 (s, 2H, -CH₂-). ESI-MS *m/z* 486 (M + H⁺).

The reaction of (**6**) with alcohol (**1**) was done in an analogous manner to the synthesis of L¹ and L³. Yield 65 %. L⁴: ¹H NMR (400MHz, CDCl₃) δ 8.70 (ddd, *J* = 4.8, 1.7, 0.9, 1H, py), 8.65 (ddd, *J* = 4.8, 1.7, 0.9, 1H, py), 8.57 (dt, *J* = 7.8, 1.1, 1H, py), 8.46 (dd, *J* = 7.8, 1.0, 1H, py), 8.33 (t, *J* = 7.2, 2H, py), 8.25 (dt, *J* = 8.1, 0.8, 2H, py), 8.21 (dd, *J* = 7.8, 0.9, 1H, py), 8.18 (s, 1H, tz), 7.93 (t, *J* = 7.8, 1H, py), 7.86 (m, 5H overlap, py), 7.60 (m, 3H, overlap, py), 7.46 (s, 1H, tz), 7.35 (ddd, *J* = 7.5, 4.8, 1.2 Hz, 1H, py) 7.26 (m, 1H, py), 4.92 (s, 2H, -CH₂-), 4.91 (s, 2H, -CH₂-), 4.90 (s, 4H, -CH₂-). ¹³C (125 MHz, CDCl₃) 169.8, 169.2, 158.5, 157.7, 157.6, 155.9, 155.6, 155.5, 155.4, 155.3, 155.2, 154.9, 152.4, 150.5, 150.4, 149.1, 149.0, 138.0, 137.6, 137.5, 137.4, 137.2, 137.1, 124.0, 122.9, 122.2, 121.7, 121.5, 121.4, 121.3, 121.1, 121.0, 119.6, 119.5, 118.7, 118.4, 73.9 (-CH₂O-), 73.6 (-CH₂O-), 73.3 (-CH₂O-), 68.7 (-CH₂O-). ESI-MS *m/z* 718 (M + H⁺).

Aromatic regions of the ^1H NMR spectra of L^1 , L^3 and L^4 are shown in Figure 1.

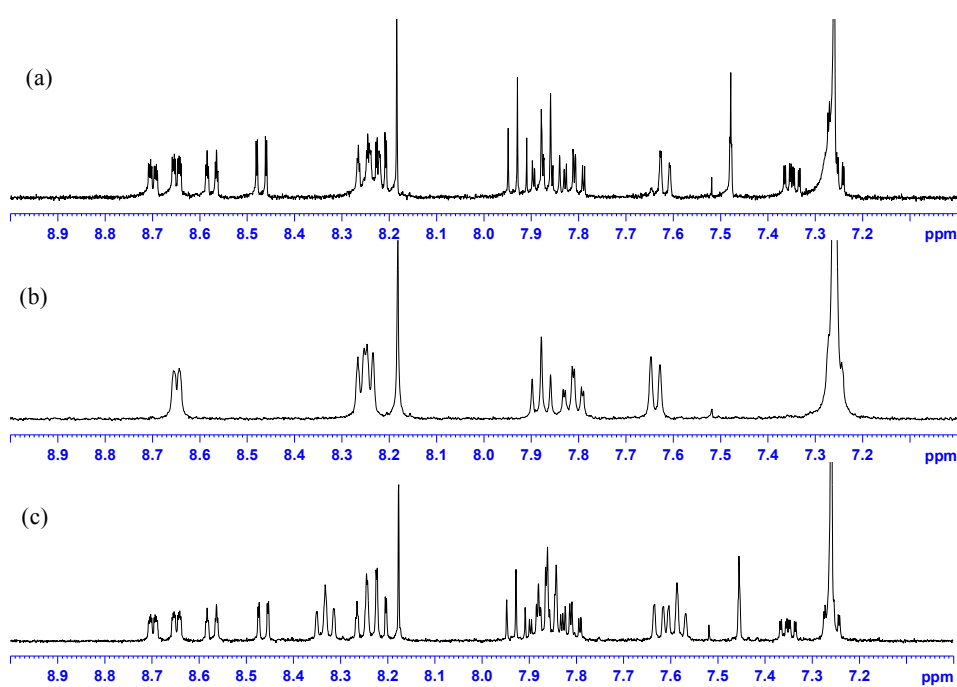


Figure 1. Aromatic regions in the ^1H NMR spectra (CDCl_3) of (a) L^1 , (b) L^3 and (c) L^4 .

Characterisation of $HH\text{-}[\text{HgZn(L}^1\text{)}_2]^{4+}$. Samples of in situ prepared $HH\text{-}[\text{HgZn(L}^1\text{)}_2]^{4+}$ complex were characterized by electrospray ionization mass spectroscopy (Figure 2) and two-dimensional ^1H NMR spectroscopy (Figures 3 and 4).

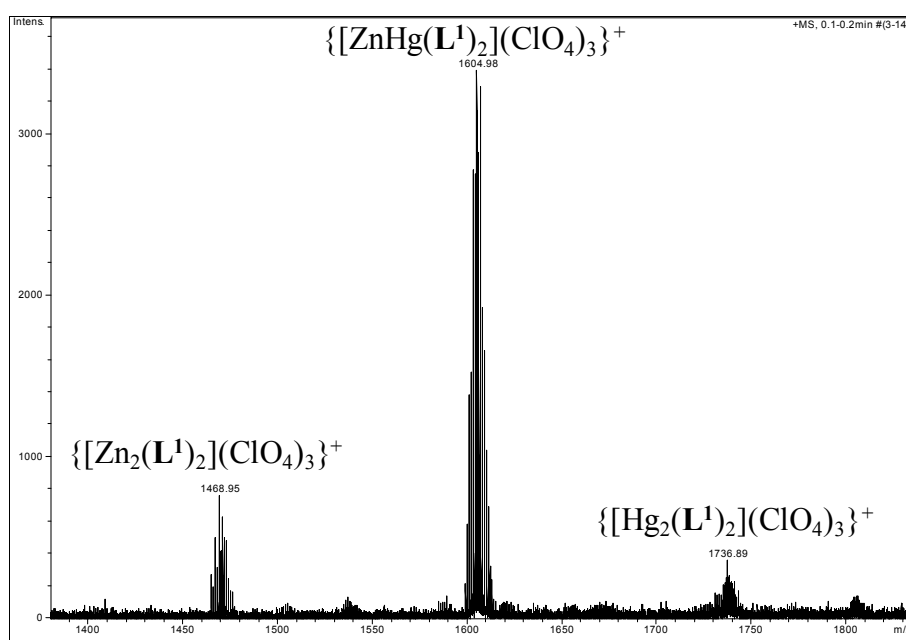


Figure 2. ESI-Mass Spectrum of the reaction of two equivalents of L^1 with one each of $\text{Hg}(\text{ClO}_4)_2 \cdot 4\text{H}_2\text{O}$ and $\text{Zn}(\text{ClO}_4)_2 \cdot 6\text{H}_2\text{O}$.

The two-dimensional spin-spin (^1H - ^1H COSY) and dipole-dipole (^1H - ^1H NOESY) NMR spectra of solutions of $HH\text{-}[\text{HgZn(L}^1\text{)}_2]^{4+}$ (CD_3CN , 500 MHz, 298 K) are shown in Figures 3 and 4, respectively, along with complete peak assignments for the aromatic protons of L^1 . Several important features in these ^1H NMR spectra support the retention of the solid-state structure of $HH\text{-}[\text{HgZn(L}^1\text{)}_2]^{4+}$ in solution and we therefore make note of the following:

- (i) The two thiazole (tz) protons (H^8 and H^{16}) appear as two well separated singlets in the one-dimensional spectra. We assign the low frequency singlet ($\delta = 7.2$ ppm) to proton H^8 based on the observation that, in the solid-state, this proton is held above the plane of an aromatic ring in the complementary ligand strand of $HH\text{-}[\text{HgZn(L}^1\text{)}_2]^{4+}$ and thus subject to shielding ring current anisotropies. We also note that satellite peaks ($J^4 = 23$ Hz) are discernible on the other, more deshielded, tz singlet ($\delta = 8.6$ ppm) due to coupling to a spin active ^{199}Hg nucleus ($I = \frac{1}{2}$, abundance 17%).⁴ The latter feature is consistent with the assignment of this peak to proton H^{16} on the tridentate py-tz-py unit.
- (ii) The majority of the remaining peak/proton assignments can be made by straightforward consideration of the peak integrals and the spin-spin coupling

correlations shown in Figure 3. In certain cases, however, there is extensive peak overlap and assignments are therefore only tentative.

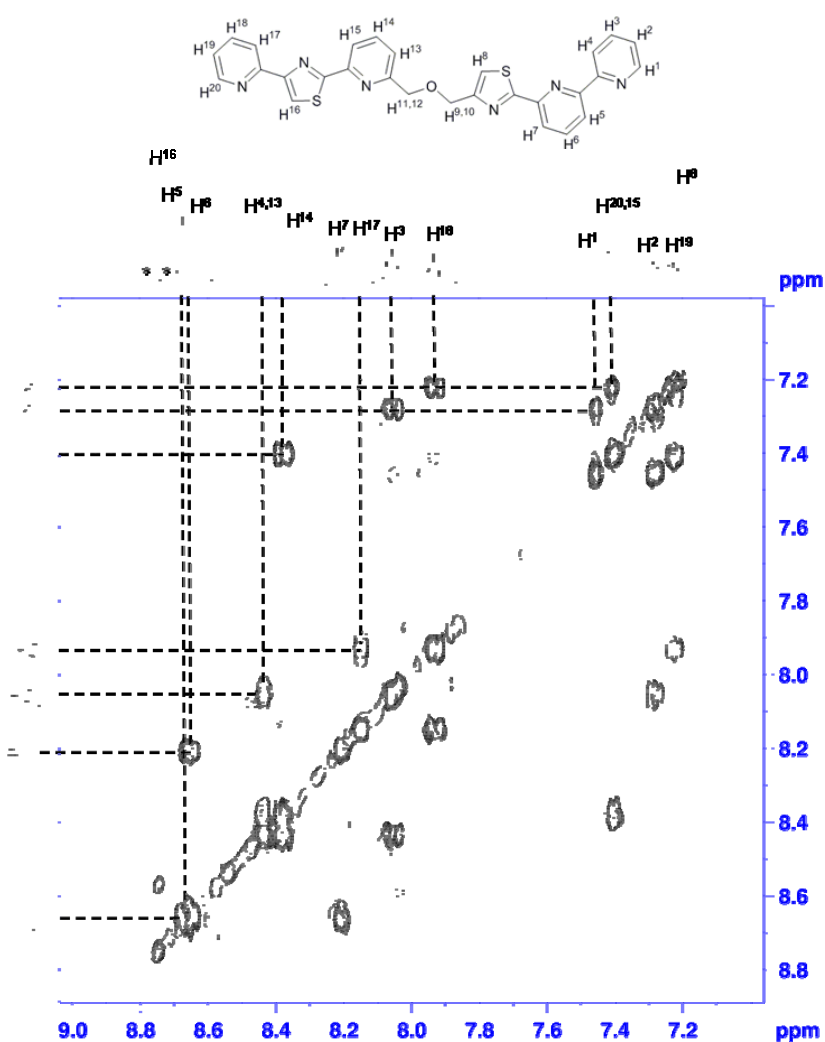


Figure 3. Aromatic region of the ${}^1\text{H}$ - ${}^1\text{H}$ COSY spectrum of $\text{HH}-[\text{HgZn}(\text{L}^1)_2]^{4+}$ in CD_3CN showing spin-spin correlations, peak assignments and proton numbering scheme. Satellites in the horizontal one-dimensional slice, due to coupling of H^{16} to the spin active ${}^{199}\text{Hg}$ isotope ($I = \frac{1}{2}$, abundance 17 %), are marked with asterisks.

- (iii) The NOESY spectra contribute little additional information regarding the structure of $\text{HH}-[\text{HgZn}(\text{L}^1)_2]^{4+}$ in solution. We observe through-space dipole-dipole interactions between proton pairs H^4/H^5 and $\text{H}^{16}/\text{H}^{17}$ as a result of *trans-trans-* to *cis-cis*-conformational changes occurring on complexation of the terminal py-py and py-tz moieties, respectively, to the metals.⁴ However, there are few through-space interactions between protons on *different* ligand strands. Only a very low intensity off-diagonal peak is present for the proton pair H^7/H^{13} .

(Figure 4), for which the non-bonded distance in the solid-state is c.a. 3 Å. We note that this is indeed the shortest inter-strand proton-proton distance in crystal structure of $HH\text{-}[\text{HgZn(L)}^1_2]^{4+}$.

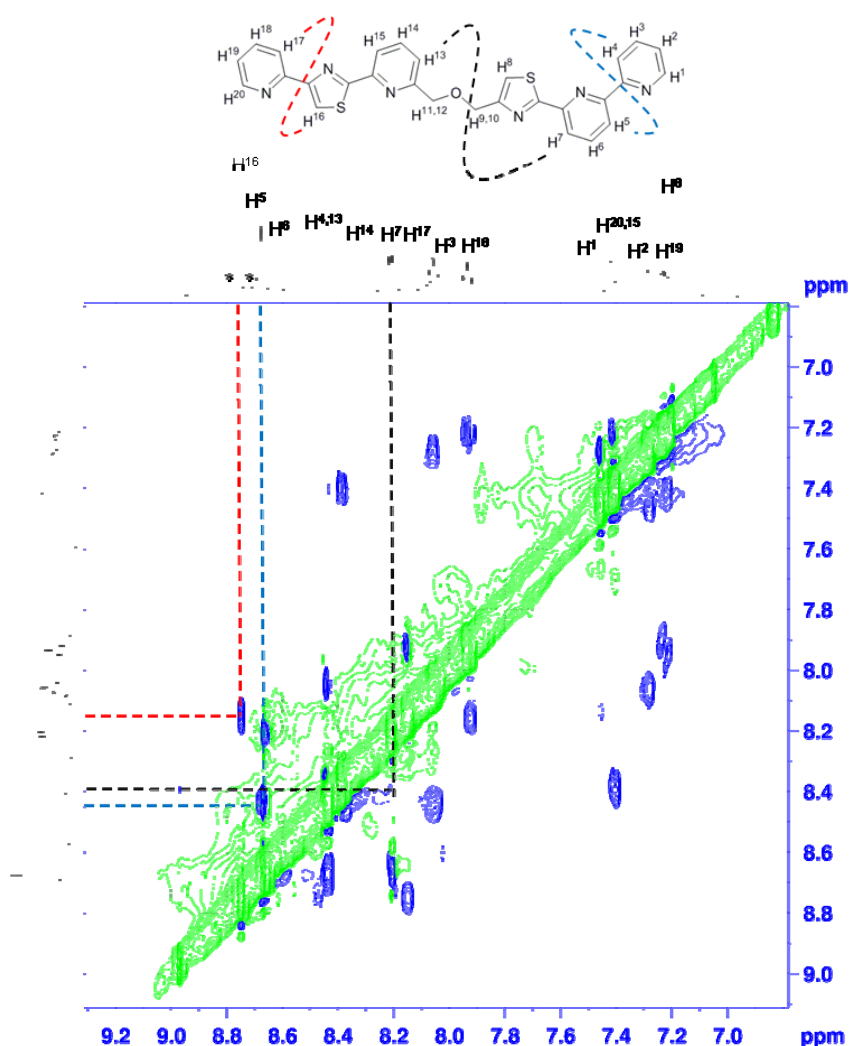


Figure 4. Aromatic region of the ^1H - ^1H NOESY spectrum of $HH\text{-}[\text{HgZn(L)}^1_2]^{4+}$ in CD_3CN showing selected through-space dipole-dipole correlations, peak assignments and proton numbering scheme. Satellites in the horizontal one-dimensional slice, due to coupling of H^{16} to the spin active ^{199}Hg isotope ($I = \frac{1}{2}$, abundance 17 %), are marked with asterisks.

Stability constant determination for complexes of L^2 . UV-Vis spectrophotometric titrations were carried out by monitoring spectral changes in the range $220 \leq \lambda \leq 420$ nm upon addition of a solution of $Zn(ClO_4)_2 \cdot 6H_2O$ or $Hg(ClO_4)_2 \cdot 4H_2O$ ($1 \cdot 10^{-3}$ M) to a solution of ligand ($2 \cdot 10^{-4}$ M) in dry acetonitrile (298 K). As is apparent in Figure 5, sequential aliquots of metal solution cause complex variations in the UV-vis spectra. Much more pronounced effects are observed during titrations with Hg^{2+} .

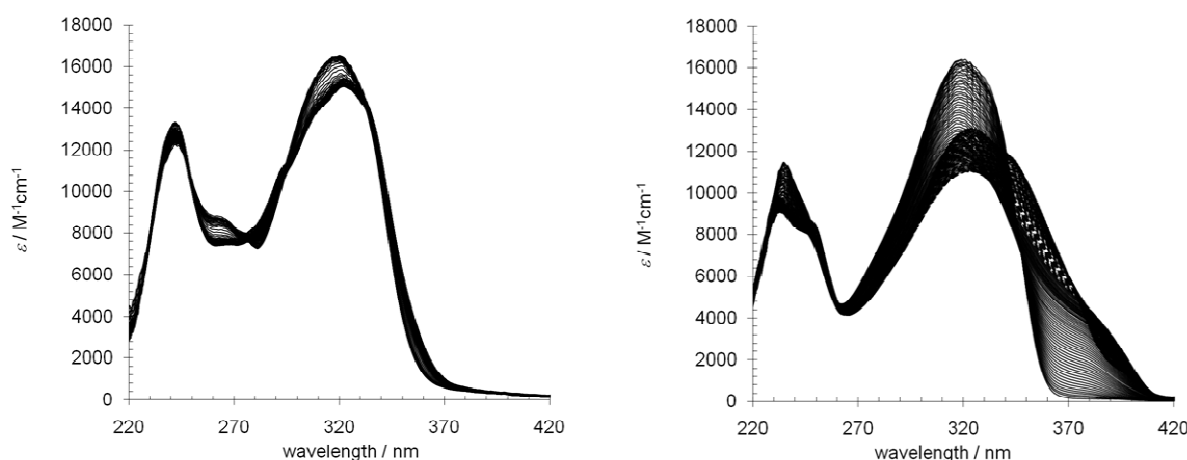


Figure 5. Variations in UV-Vis spectra observed upon addition of $Zn(ClO_4)_2 \cdot 6H_2O$ (left) or $Hg(ClO_4)_2 \cdot 4H_2O$ (right) to solutions of L^2 in MeCN (298 K).

Inflection points can be seen in the plots of absorbance vs metal/ligand ratio at $M/L \approx 0.3$ and 0.5 (Figure 6), but only for Hg^{2+} do the spectra evolve up to $M/L \approx 1.0$, after which a constant reduction in absorbance results simply from continued dilution. Accordingly, for Zn^{2+} the data was satisfactorily fitted to a model which considers only the three absorbing species in equilibria 1 and 2:



For the Hg^{2+} titration, however, evolving factor analysis¹ suggested the presence of four absorbing species and the data was therefore fitted to a more complex model which considers the formation of the same three absorbing species observed in titrations with Zn^{2+} (eq. 4, 5), in addition to the 1:1 complex formed in equilibrium 3.



In both cases, multiple non-linear least-squares fitting of the models to the data converged with excellent residuals and yielding chemically sensible absorption spectra.

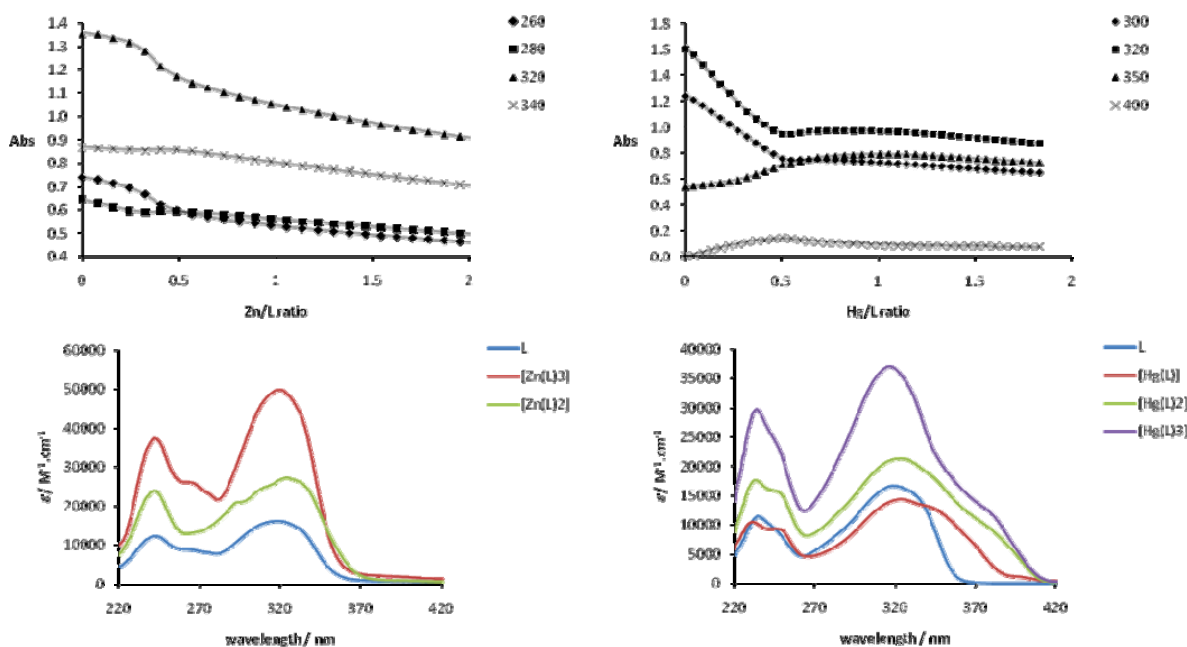


Figure 6. Plots of absorbance vs metal/ligand ratio for four selected wavelengths in the UV-Vis titrations of Zn^{2+} (top left) and Hg^{2+} (top right) into solutions of L^2 (the line represents the best fit), and calculated spectra (bottom) of the complexes included in the speciation models.

Crystallographic refinement details for $HH\text{-}[Hg_{1.29}Zn_{0.71}(L^1)_2][ClO_4]_4\cdot 2Et_2O\cdot 1.42MeCN$. Disorder present in the complex cation is caused by one of the metal sites being occupied by Zn in ca. 71 % of the crystal and Hg in the remaining ca. 29 % of the crystal (these values correspond to refined population parameters). The two terminal py-py units which constitute this site thus alternate between two positions; one in which metal-ligand bonds are relatively short (bonding to Zn) and one in which metal-ligand bonds are relatively long (bonding to Hg). The coordinates and ADPs of the metals were constrained to be equal (EXYZ and EADP) and their population parameters refined against a free variable which converged to ca. 0.71. The population parameters of the two disordered py-py units were kept identical to those of their corresponding metal and their geometries were restrained using a regime of similarity (SAME), co-planarity (FLAT) and distance (DFIX) restraints. The displacement parameters were refined anisotropically, but constrained (EADP) to be identical to those of the same atom in the other component. Regarding interstitial solvate and anion moieties, of the two crystallographically independent perchlorate anions, one was sufficiently disordered to merit resolving into two components, the population parameters of which converged at 0.27:0.73. The coordinates of each component were introduced using a non-disordered ClO_4^- fragment from the CSD

(FRAG/FEND) and both were further refined as rigid bodies (AFIX 9). The site-occupancy of a partially resolved MeCN molecule was refined against a free variable which converged to 0.71. The molecule was refined isotropically and without positional or displacement parameters restraints. Finally, a suspect molecule of Et₂O was identified in the Fourier difference map, but owing to severe disorder, its scattering contributions were removed using the SQUEEZE routine in PLATON.⁵ The additional solvates expressed in the complex formula HH-[Hg_{1.29}Zn_{0.71}(L¹)₂][ClO₄]₄·1.42MeCN·2Et₂O reflect the estimated number of Et₂O moieties (per complex unit) and are consistent with a residual electron density count of ca. 236 electrons per unit cell.

Crystallographic refinement details for [Zn₂(L²)₂][ClO₄]₄·3MeCN·Et₂O. Of the four crystallographically independent perchlorate anions, one was sufficiently disordered to merit resolving into two components, the population parameters of which were refined against a free variable (converged to 0.58:0.42). Each component was refined with isotropic displacement parameters and no geometric restraints. Three suspect MeCN and one Et₂O molecule were located in the difference map, but owing to extensive disorder, attempts at modeling only one MeCN were made. The latter was assigned two positions (population parameters refined against a free variable to 0.67:0.33), the coordinates of which were introduced from ordered MeCN moieties in the CSD and further refined as rigid bodies. The scattering contributions from the remaining interstitial solvents were removed using the SQUEEZE routine in PLATON.⁵ The additional solvates expressed in the complex formula [Zn₂(L³)₂][ClO₄]₄·3MeCN·Et₂O reflect the estimated number of solvate moieties per complex unit and are consistent with a residual electron density count of ca. 200 electrons per unit cell.

References

- 1 (a) H. Gampp, M. Maeder, C. J. Meyer and A. D. Zuberbühler, *Talanta* 1985, **23**, 1133-1139; (b) H. Gampp, M. Maeder, C. J. Meyer and A. D. Zuberbühler, A. D. *Talanta* 1986, **33**, 943-951; (c) M. Maeder and Y.-M. Neuhold, in *Practical Data Analysis in Chemistry*; S. Rutan and B. Walczak, Eds.; Elsevier Publishing Co.: Amsterdam, 2007.
- 2 T. Riis-Johannessen, Lindsay P. Harding, John. C. Jeffery, Ryan Moon and Craig R. Rice, *Dalton Trans.*, 2007, 1577-1587.
- 3 G. R. Newkome, W. E. Puckett, G. E. Kiefer, V. K. Gupta, Y. Xia, M. Coreil and M. A. Hackney, *J. Org. Chem.*, 1982, **47**, 4116.
- 4 T. Riis-Johannessen, John. C. Jeffery, Alex P. H. Robson, Craig R. Rice and Lindsay P. Harding, *Inorg. Chim. Acta*, 2005, **358**, 2781 and references cited therein.
- 5 A. L. Spek, *Acta Cryst. C*, 1990, **A46**, C-34; PLATON – A Multipurpose Crystallographic Tool; Utrecht University, Utrecht, The Netherlands, A. L. Spek, 2003.